Biophysical Chemistry, 33 (1989) 177–193
Elsevier

BPC 01353

Subunit flow in F-actin under steady-state conditions

Application of a novel method to determination of the rate of subunit exchange of F-actin at the terminals

Naoya Suzuki and Koshin Mihashi

Laboratory of Molecular Biophysics, Department of Physics, Faculty of Science, Nagoya University, Chikusa-ku, Nagoya 464-01, Japan

Received 1 November 1988
Revised manuscript received 20 January 1989
Accepted 23 January 1989

Actin, F-; Subunit exchange, steady-state; Treadmilling; Pyrenyl-actin; Subunit flow

We developed a novel method to determine the subunit exchange rates of F-actin at its terminals under quasi-steady-state conditions by using a powerful fluorescent probe, *N*-(1-pyrenyl)iodoacetamide. The applicability of the method was checked with regard to both theoretical and experimental aspects. We determined the rates of subunit exchange of F-actin and F-actin-tropomyosin complex under various ionic conditions. We found that: (i) KCl accerated both on and off rates at each end, and lowered the critical concentration of the P-end while the critical concentration of the B-end was not affected; (ii) binding of tropomyosin drastically reduced the subunit flow in F-actin by suppressing the off rate principally of the P-end. It is therefore believed that tropomyosin exerts an anisotropic constraint on F-actin and regulates its dynamic polarity.

1. Introduction

1.1. Subunit flow in F-actin under steady-state conditions

It has been demonstrated that, in the presence of ATP, the critical concentration of the terminals of F-actin differ [1]. The critical concentrations of the B-end (barbed-end) is much lower than that of the P-end (pointed-end), indicating that the free energy change associated with binding of G-actin to the terminal is different between the terminals. In contrast, the frequency of subunit association and dissociation at the terminal of F-actin is at least several times higher at the B-end as compared to the P-end [2,3]. The disparity in critical concentrations between the B-end and P-end of F-actin described above suggests that subunit flow takes place in F-actin under steady-state conditions in the presence of ATP. In an experimental and theoretical work presented several years ago by Wegner [4], the suggestion was put forward as to the existence of directional subunit flow in F-actin under steady-state conditions (for recent reviews, see refs. 5 and 6).

In order to demonstrate steady-state subunit flow in F-actin and to investigate the quantitative aspects of modulation of subunit flow by actin-binding regulatory proteins under various ionic conditions, we developed a novel method in which use is made of a powerful fluorescent probe attached to a specified site of the actin polypeptide described in a previous paper [7]. By means of this new, sensitive technique, we measured incorporation of label into F-actin under quasi-steady-state (growing) conditions with a threshold of detection as low as a few subunits/filament. The unique advantage of this method is that it is not necessary

Correspondence address: N. Suzuki, Laboratory of Molecular Biophysics, Department of Physics, Faculty of Science, Nagoya University, Chikusa-ku, Nagoya 464-01, Japan.
Abbreviation: PIAA, *N*-(1-pyrenyl)iodoacetamide.

to modify F-actin artificially for identification of its polarity, for example, by fixation with cross-linking reagents (glutaraldehyde, etc.) or decoration with myosin head, as was required in previous studies [2,3]. Any artificial treatment of F-actin, such as chemical cross-linking or decoration with other proteins, may lead to a change in the dynamics of subunit exchange at the terminals. In fact, a significant finding in the present study is that the subunit flow in F-actin is very susceptible to binding of actin-related proteins.

1.2. Uncertainty in steady-state concentration of G-actin in F-actin solution due to heterogeneity of the terminal nucleotide

Polymerization of G-actin-ATP is associated with ATP hydrolysis [8]. However, the hydrolysis of ATP is not tightly coupled with the incorporation of G-actin-ATP into the terminal of F-actin, but occurs on F-actin in a stochastic manner [9,10]. Therefore, if the filament is in a growth phase where the rate of addition of G-actin to the F-actin end is greater than that of ATP hydrolysis on F-actin, accumulation of ATP-binding subunits may occur at the terminal [10,11]. On the other hand, if the filament is in a contraction phase, most of the terminal subunit binds ADP. Therefore, under steady-state conditions, the nucleotide bound to the terminal actin subunit may vary among ATP and ADP (or ADP plus P_i [12]) in a stochastic way.

It has been shown previously that the on/off rate of actin subunits at F-actin terminals differs between ATP- and ADP-actin [13,14]. Therefore, the on/off rate of the terminal subunit of a single actin filament under steady-state conditions will fluctuate spontaneously, and the on/off rate constants determined in the present work are the statistical values averaged in a population of F-actin with heterogeneous terminal nucleotides.

2. The principle of incorporation of labeled G-actin into F-actin under quasi-steady-state conditions

2.1. Elementary reaction

In the presence of sufficient G-actin, F-actin grows at both B- and P-ends. The rate of elongation at one end is given by the number of subunits that bind per unit time (t) to that end. This equals the difference in frequency between the association $k^+C(t)$ and dissociation k^- of actin subunits at the terminal:

$$V_B(t) = k_B^+ C(t) - k_B^- \tag{1-1}$$

$$V_P(t) = k_P^+ C(t) - k_P^- \tag{1-2}$$

where k^+ and k^- are the corresponding association and dissociation constants for each end, and $C(t)$ the monomer concentration at time t. The total growth rate of a single filament is the sum of the contributions from both ends:

$$V_{B+P}(t) = (k_B^+ + k_P^+)C(t) - (k_B^- + k_P^-) \tag{2}$$

2.2. Approach to steady state

As the reaction proceeds, $C(t)$ decreases with time. Finally, a steady state is attained where no net growth of filaments occurs on average; $V_{B+P} = 0$. The steady-state concentration of G-actin, C_s, is thus related to the rate constants as follows:

$$C_s = (k_B^- + k_P^-)/(k_B^+ + k_P^+) \tag{3}$$

2.3. Structure of the steady state

We obtain an expression relating the reactions at both opposite terminals (B- and P-ends) under the steady-state condition of eq. 3:

$$(k_B^+ C_s - k_B^-) = -(k_P^+ C_s - k_P^-) \tag{4}$$

The numerical value of this equation is not necessarily equal to zero, but can be positive, negative or zero, depending on the combination of the four rate constants.

In the case where eq. 4 takes a positive value, the B-end will grow in length such that the P-end will shorten at the same speed. This represents a typical example of 'treadmilling', as originally suggested by Wegner [4]. In contrast, if the value of eq. 4 is negative, the B-end becomes shorter at the same rate as that of lengthening of the P-end. However, this case has not been demonstrated as yet for F-actin [2,3]. When eq. 4 is equal to zero, net growth is observed at neither the B-end nor P-end.

2.4. Critical concentrations of both ends and steady-state concentration of G-actin

The critical concentrations of the B- and P-ends are defined as follows;

$$C_B = k_B^-/k_B^+ \quad (5)$$

$$C_P = k_P^-/k_P^+ \quad (6)$$

The steady-state structure can be described in terms of the critical concentrations of both ends and the steady-state concentration as follows;

$$C_B < C_s < C_P \quad (7)$$

$$C_B > C_s > C_P \quad (8)$$

$$C_B = C_s = C_P \quad (9)$$

Therefore, one can see that simple diagnosis of the occurrence of treadmilling (eqs. 7 and 9) involves determination of whether the critical concentrations of the B- and P-ends differ.

2.5. Quasi-steady-state determination of rate constants of subunit exchange at the terminals of F-actin

On the basis of the above consideration, we wish to develop a new method for determination of the on/off rate constants of subunit exchange at both terminals of F-actin under quasi-steady-state conditions.

Let us consider the case of addition of a small amount of labeled G-actin (C_0) to a solution of F-actin (unlabeled) at the steady state of subunit exchange. If we choose the value of C_0 such that the ratio of C_0 to C_s is sufficiently less than unity ($C_0/C_s \ll 1$), the solution is in a quasi-steady state. Under this condition, excess G-actin is preferably incorporated into F-actin rather than contributing to autonomic polymerization (nucleation). Therefore, the threshold for the amount of labeled G-actin to be added should be determined under each experimental condition.

Depending on the magnitudes of C_B (or C_P) and C_s, the kinetics of incorporation of label into F-actin are described separately (eqs. 7 and 9).

2.5.1. Case A: $C_B = C_s = C_P$

In this case, under quasi-steady state conditions after addition of label, elongation occurs at both ends of F-actin (B- and P-ends). If no preferential incorporation occurs between labeled and unlabeled G-actin, the rate of label incorporation into single F-actin is given as follows:

$$V^*_{B+P}(t) = A(t)\left[(k_B^+ + k_P^+)C(t) - (k_B^- + k_P^-)\right] \quad (10)$$

where $A(t)$ is the fraction of labeled G-actin in the total G-actin at time t. If the fluorescence increase of the label is the same at both ends of F-actin, the fluorescence intensity of the solution $FI_{B+P}(t)$ increases according to:

$$\frac{dFI_{B+P}(t)}{dt} = fPA(t)\left[(k_B^+ + k_P^+)C(t) - (k_B^- + k_P^-)\right] \quad (11)$$

where P is the number concentration of actin filaments and f the proportionality constant between the fluorescence intensity and the concentration of label in F-actin. (We may note again that the rate constants given above are averages for a heterogeneous population of nucleotide at the terminal actin subunits, ADP, ATP and ADP plus P_i.) In the case where the B-end is capped with actin-binding protein or cytochalasins [15] which suppresses subunit exchange at the terminal, the observed rate of the fluorescence increase is

$$\frac{dFI_P(t)}{dt} = fPA(t)\left[k_P^+ C(t) - k_P^-\right] \quad (12)$$

In the present method, the fluorescence change was initiated by adding a small amount (about 50 μl) of labeled G-actin to 2 ml F-actin solution (unlabeled) in a test tube. The solution was then gently mixed and decanted into a cuvet for fluorescence measurement. These processes took at least 10–15 s. It is important to note that during the very early stage after addition of labeled G-actin, the rate of label incorporation did not follow eq. 10, since the terminal subunits of most actin filaments had not yet been labeled. Instead, label incorporation is described by the following association reaction only (without dissociation terms):

$$V^*_{B+P}(t \to 0) = A(0)\left[(k_B^+ + k_P^+)C(0)\right] \quad (10')$$

As incorporation of label proceeds and labeled subunit is accumulated at the terminal of F-actin,

dissociation of labeled subunit from the terminal becomes significant relative to association of label with the terminals. At this stage, the rate of label incorporation is well described by eq. 10. Therefore, it is necessary to select an appropriate time domain for label incorporation in which eq. 10 is valid to a good approximation. Determination of the appropriate time domain was carried out by computer simulation of the process of label incorporation (appendix A). After this analysis, we found that the rate of fluorescence increase averaged for the time domain between 50 and 120 s after addition of labeled G-actin provides a good approximation of the rate described in eq. 10. That is, the rate of fluorescence increase in this time domain is expressed in terms of the initial total G-actin concentration $C(0)$ and the initial fraction of labeled G-actin $A(0)$ as follows:

$$\left.\frac{\mathrm{dFI_{B+P}}(t)}{\mathrm{d}t}\right|_{t\to 0} = fPA(0)\left[(k_B^+ + k_P^+)C(0) - (k_B^- + k_P^-)\right] \quad (13)$$

$$\left.\frac{\mathrm{dFI_P}(t)}{\mathrm{d}t}\right|_{t\to 0} = fPA(0)\left[k_P^+ C(0) - k_P^-\right] \quad (14)$$

where $C(0) = C_s + C_0$ and $A(0) = \alpha C_0/(C_s + C_0)$. C_0 represents the concentration of G-actin added and α the fraction of labeled G-actin added to F-actin solution.

After addition of labeled G-actin, the total G-actin concentration $C(t)$ approaches a value very close to C_s, and the fraction of labeled G-actin in total G-actin $A(t)$ decreases. Thus, the rate of fluorescence change decreases gradually. As described in appendix A, we observed that the relationships of eqs. 13 and 14 are good approximations of the fluorescence increase during the early stage where the amount of the incorporated labeled G-actin is no greater than 5% of the initial total G-actin (labeled plus unlabeled). We can transform eqs. 13 and 14 as follows:

$$\frac{1}{A(0)}\left.\frac{\mathrm{dFI_{B+P}}(t)}{\mathrm{d}t}\right|_{t\to 0} = fP\left[(k_B^+ + k_P^+)(C_s + C_0) - (k_B^- + k_P^-)\right] \quad (15)$$

$$\frac{1}{A(0)}\left.\frac{\mathrm{dFI_P}(t)}{\mathrm{d}t}\right|_{t\to 0} = fP\left[k_P^+(C_s + C_0) - k_P^-\right] \quad (16)$$

Eqs. 15 and 16 demonstrate that when the initial steady rate of fluorescence increase normalized by $A(0)$ for a given C_0 is plotted vs. total G-actin $(C_s + C_0)$, we obtain a straight line whose slope is proportional to the association rate constant (k^+) and whose intercept on the ordinate is proportional to the dissociation rate constant (k^-).

The proportionality constants (fP) are given as follows. f depends on the experimental conditions and is calculated from a combination of the steady-state value of the fluorescence increase and the steady-state concentration of label incorporated into F-actin. This is given approximately as the product of the initial label concentration (αC_0) and the fraction of actin subunit in F-actin relative to total actin; $(C_{tot} + C_0 - C_s)/(C_{tot} + C_0)$.

$$\mathrm{FI}(t \to \infty) = f\alpha C_0 \frac{C_{tot} + C_0 - C_s}{C_{tot} + C_0} \quad (17)$$

On the other hand, P (the number concentration of F-actin) is determined by labeling the B-end of F-actin with [^{3}H]cytochalasin B as tracer.

The variable parameter in this experiment is C_0; the concentration of added G-actin (labeled plus unlabeled). The initial velocity of the fluorescence increase divided by $A(0)$; $[\{\mathrm{dFI}(t)/\mathrm{d}t\}_{(t\to 0)}/A(0)]$ is plotted as a function of total G-actin $(C_s + C_0)$ according to eqs. 15 and 16. The on/off rate constants of the P-end are determined according to eq. 16, and then by substituting the results for the P-end into eq. 15, the on/off rate constants of the B-end are determined.

2.5.2. Case B: $C_B < C_s < C_P$

In the case where the difference between the critical concentrations of the B- and P-ends is significantly large, we can add C_0 such that it satisfies the relation $(C_s + C_0) < C_P$. Under these conditions, incorporation of label occurs exclusively at the B-end (appendix A), and the fluorescence increase during the early stages of label incorporation ($t \simeq 0$) is related to the on/off rate

constants of the B-end as follows;

$$\frac{1}{A(0)}\frac{\mathrm{dFI}(t)}{\mathrm{d}t}\bigg|_{t\to 0} = fP\left[k_B^+(C_s + C_0) - k_B^-\right] \quad (18)$$

As for case A, a plot of $[\{\mathrm{dFI}(t)/\mathrm{d}t\}_{(t\to 0)}/A(0)]$ vs. $(C_s + C_0)$ gives the on/off rate constants of the B-end.

The on/off rate constants of the P-end can be determined via two independent ways. The first involves insertion of both on/off rate constants of the B-end obtained above and the critical concentration of P-end into the following relations which are obtained from eqs. 3 and 6.

$$k_P^+ = \frac{k_B^+ C_s - k_B^-}{C_P - C_s} \quad (19)$$

$$k_P^- = k_P^+ C_P \quad (20)$$

The second consists of measuring the rate of label incorporation shortly after addition of the B-end capping protein (or cytochalasin D [15]). In this case, the observed rate of label incorporation is expressed by the following relation which is identical to eq. 16;

$$\frac{1}{A(0)}\frac{\mathrm{dFI}_P(t)}{\mathrm{d}t}\bigg|_{t\to 0} = fP\left[k_P^+(C_s + C_0) - k_P^-\right] \quad (21)$$

Eq. 21 is applicable in the time domain shortly after addition of cytochalasin D and before the change in critical concentration (from C_s to C_P due to capping of the B-end by cytochalasin D) becomes significant.

3. Experimental

3.1. Chemicals and materials

[^{3}H]Cytochalasin B (18.5 Ci/mmol) was purchased from New England Nuclear. ^{3}H was incorporated into a nonexchangeable position of cytochalasin B [18]. Cytochalasin B (unlabeled) and cytochalasin D were purchased from Aldrich. These cytochalasins were stored in dimethyl sulfoxide at 4°C. *N*-(1-Pyrenyl)iodoacetamide was purchased from Molecular Probes. Scintisol EX-H, hydroxyapatite and ATP were purchased from Dojin, Wako and Sigma, respectively. All other chemicals were of reagent grade.

A Hitachi 65P apparatus was used for centrifugal separation of proteins. Fluorescence measurements were recorded on a Hitachi MPF-2A spectrofluorimeter equipped with a Haake thermobath which maintained cuvet temperature to within ±0.2°C. An Aloka 1000 liquid scintillation counter was used to determine ^{3}H radioactivity.

Computer simulation was carried out using the facilities of the Nagoya University Computation Center.

3.2. Proteins and fluorescence labeling of actin

Actin from rabbit skeletal muscle was prepared in the same way as in the previous work [7]. The purified F-actin was dialyzed against a large volume of solution A which contained 100 mM KCl, 2 mM $MgCl_2$, 50 μM $CaCl_2$, 200 μM ATP, 1 mM $NaHCO_3$, 1 mM NaN_3 at 5°C. Tropomyosin was prepared according to methods described previously [16,17]. F-Actin-tropomyosin complex was prepared as follows. Firstly, tropomyosin was mixed with G-actin in a 1:5 molar ratio in low ionic strength buffer (200 μM ATP, 100 μM $CaCl_2$, 2 mM $NaHCO_3$ and 2 mM 2-mercaptoethanol). The mixture was dialyzed against high ionic strength buffer (100 μM ATP, 60 mM KCl, 2 mM $MgCl_2$, 15 mM Tris-acetate (pH 7.6) and 2 mM 2-mercaptoethanol) at 5°C overnight to polymerize actin. The solution of F-actin-tropomyosin complex obtained was further dialyzed with the appropriate solution for each set of experimental conditions before use.

Fluorescence labeling of F-actin with *N*-(1-pyrenyl)iodoacetamide (PIAA) was performed according to the method in ref. 7, with the following slight modification. PIAA was dissolved in *N*,*N*-dimethylformamide (DMF) giving a concentration of 1–3 mM. Before mixing with F-actin, PIAA in DMF was diluted with solution A resulting in a PIAA concentration of the order of 50–100 μM. 1 vol. of this solution was carefully added to

2 vols F-actin (20–30 μM) in solution A at 0 °C. The mixture was gently stirred at 0 °C in the dark for 6 h. The reaction was then stopped by adding 2-mercaptoethanol to 3 mM. The solution was centrifuged at low speed (6000 × g for 30 min) to remove unreacted precipitates of PIAA. Subsequently, the labeled F-actin was centrifuged at high speed (20000 × g) for 70 min. The pellets of labeled F-actin were dissolved in buffer G containing 200 μM ATP, 100 μM $CaCl_2$, 1 mM $NaHCO_3$, 3 mM 2-mercaptoethanol and 1 mM NaN_3. The solution was then dialyzed against a large volume of buffer G. Finally, the solution was purified by centrifugation at 10000 × g for 30 min. About 70–95% of actin was labeled with PIAA by this method.

3.3. ATPase assay

1 ml of each sample solution was separated and an equal volume of perchloric acid (12%) was added in ice to precipitate proteins. The solution was passed though a filter paper to remove protein precipitates. The filtrate was then neutralized with KOH. The content of nucleotides in the solution was analysed by HPLC on a TSK gel (DEAE-2SW, Toyo Soda) of size 4.6 mm × 25 cm at a pressure of 120 kg/cm^2.

3.4. Measurement of the critical concentration of actin

The critical concentration of actin was determined using the method of Kouyama and Mihashi [7] employing the fluorescent probe, PIAA which labeled the Cys-374 residue of the actin peptide. The fluorescence intensity (excitation at 365 nm and emission at 405 nm) of PIAA-labeled actin is enhanced approx. 25-times when labeled G-actin is incorporated into F-actin [7]. G-Actin solution (containing 5% pyrenyl-actin and, if necessary, tropomyosin at 1:5 molar ratio to actin) was diluted with buffer G. Cytochalasin D (1 μM) was added when the critical concentration of the P-end was measured. Polymerization of actin was induced by adding $MgCl_2$ (1 mM) or $MgCl_2$ (1 mM) plus KCl (30 or 60 mM). This solution was warmed to 31 °C and allowed to stand for about 4 h to attain a steady state. The steady-state G-actin concentration (critical concentration) was then determined by measuring the fluorescence intensity.

3.5. Measurement of cytochalasin B binding to F-actin

The number concentration of F-actin was determined by measuring the concentration of cytochalasin B-binding sites in F-actin solution by making use of the ability of cytochalasin B to bind strongly to the B-end of F-actin [15]. F-Actin (10.0 μM, 4.0 ml) was incubated in a solution containing 20 mM KCl, 1 mM $MgCl_2$, 20 mM Tris-HCl (pH 8.0), 100 μM $CaCl_2$, 200 μM ATP, 1 mM NaN_3 and 0.5 mM 2-mercaptoethanol (solution F) at 30 °C for 20 min. A trace amount of diluted [^{3}H]cytochalasin B (0.29 μCi/ml) was added to several F-actin solutions in which the concentration of cytochalasin B was between 4 and 100 nM. After gentle mixing of the protein with cytochalasin B, the solutions were centrifuged at 220000 × g for 60 min at 25 °C to remove protein-bound radioactivity from free cytochalasin B. The supernatants were decanted into another test tube and the pellets in the centrifuge tubes were washed gently using solution F without homogenization to remove the remaining supernatant. The pellets were then dissolved in solution G (F solution from which KCl and $MgCl_2$ were omitted). Given amounts of both supernatants and pellets dissolved in solution G were homogenized with scintillator EX-H, and the radioactivity in each solution was counted. The amounts of both protein-bound and free cytochalasin B were analysed in terms of Scatchard plots.

3.6. Measurement of the rate of label incorporation

The principle outlined in section 2 was applied to analysis of subunit exchange of F-actin under conditions close to steady state. We used the fluorescent probe, PIAA to label Cys-374 of the actin peptide [7]. With this probe, we could detect subunit association of as little as a few subunits/filament. The experimental procedure is as follows.

F-Actin solution (or F-actin-tropomyosin complex solution) containing 10 μM actin in the test

tube was incubated for 30 minutes at 31° C. Pyrene-labeled G-actin was added to the test tube at a level as low as a few micromolar and mixed gently upside-down. The F-actin solution was decanted into a fluorescence cuvet and the fluorescence was measured. About 20 s elapsed from the addition of labeled G-actin to the measurement of fluorescence. To measure the rate of label incorporation at the P-end, cytochalasin D (0.5 μM) was added 2 min before addition of labeled G-actin.

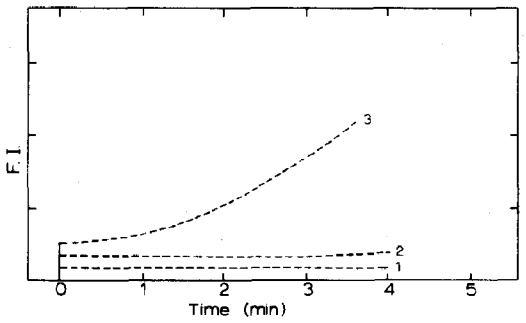

Fig. 1. Threshold of G-actin concentration for spontaneous polymerization. At $t = 0$, various amounts of G-actin (5% labeled) were added to 'K/Mg' solution containing 30 mM KCl, 1 mM $MgCl_2$, 50 μM $CaCl_2$, 5 mM Tris-HCl (pH 8.0), 200 μM ATP, 1 mM NaN_3 and 1 mM 2-mercaptoethanol at 31° C, and the fluorescence intensity (F.I.) of the labeled probe was continuously monitored. Final concentrations of G-actin added were (1) 1.0 μM, (2) 2.0 μM, (3) 2.9 μM. Note that, under the solvent conditions described above, there was no detectable polymerization during the early time domain (until 4 min after addition of G-actin), provided that the concentration of G-actin did not exceed 2 μM. The rate of label incorporation was determined in the time domain between 1 and 2 min after addition of labeled G-actin (see appendix A).

4. Results

4.1. Limitation of the amount of labeled G-actin added in order to avoid spontaneous polymerization

In applying the new method, it is essential to avoid spontaneous nucleation of G-actin. Therefore, we need to know the threshold value of the G-actin concentration under those conditions where spontaneous polymerization becomes detectable within the experimental time (usually less than 5 min).

Under the conditions of ionic composition 1 mM $MgCl_2$, 30 mM KCl, 50 μM $CaCl_2$, 5 mM Tris-HCl (pH 8.0), 200 μM ATP, 1 mM NaN_3, 1 mM 2-mercaptoethanol, 31° C, spontaneous polymerization was not detected up to 2 μM added labeled G-actin (fig. 1). Therefore, in the following experiments on rate determination carried out under conditions of 1 mM $MgCl_2$ plus KCl (0, 30, 60 mM) where the steady-state concentration of G-actin was around 0.5 μM, labeled G-actin at less than 1.5 μM was added to 10 μM F-actin solution.

4.2. Determination of steady-state concentration of G-actin under the experimental conditions

4.2.1. Time of attaining steady state for subunit exchange of F-actin

In application of the new method, we need to determine the critical concentration of actin in both the presence (C_P) and absence (C_s) of cytochalasin D (eqs. 3 and 6). In such determination, it is essential that a true steady state is established. Attainment of a steady state for the polymerization-depolymerization of actin is proved if the concentration of G-actin which coexists with F-actin is the same in both solutions, one commencing with G-actin and the other with F-actin.

For this purpose, labeled G-actin was mixed with unlabeled G-actin at a molar ratio of 0.05, and the solution was divided into two halves. The first half was multiply diluted with buffer G in test tubes. Then actin was polymerized by adding $MgCl_2$ and KCl to 1 mM and 60 mM, respectively. After being kept at 5° C for 2 days, the solutions were incubated at 31° C for 5 h and the F-actin in each test tube was assayed by measuring the fluorescence intensity of the solution (fig. 2). In the other half, G-actin was firstly polymerized by adding KCl and $MgCl_2$ (60 mM and 1 mM, respectively) and then multiply diluted with buffer F containing 60 mM KCl, 1 mM $MgCl_2$, 50 μM $CaCl_2$, 200 μM ATP, 5 mM Tris-HCl (pH 8.0), 1 mM NaN_3 and 1 mM 2-mercaptoethanol. After being kept at 5° C for 2 days, solutions were incubated at 31° C for 5 h before fluorescence measurement.

The steady-state G-actin concentration thus determined was 0.5 ± 0.1 μM irrespective of the sequence dilution → polymerization or polymerization → dilution.

The same procedure was followed in the presence of cytochalasin D. Since cytochalasin D is known to 'cap' the B-end [15] where subunit exchange is more frequent than at the opposite end, the time required to attain a steady state is longer in the presence of cytochalasin D than its absence. We found that the steady-state G-actin concentration in the presence of cytochalasin D was 2.8 ± 0.1 μM irrespective of the sequence of dilution-polymerization (fig. 2). This indicates that a steady state in the presence of cytochalasin D was established in less than 2 days. We then attempted to ascertain the conditions for establishing a steady state in a shorter time (or to give the same steady-state G-actin concentration), and found finally that the steady state could be achieved in a preparation where G-actin was multiply diluted and polymerized at 31° C, and then incubated at 31° C for 4 h. Although the minimum time required for the solution to reach a steady state may be less than 4 h at 31° C, the steady-state G-actin concentrations under several ionic conditions were determined in this way.

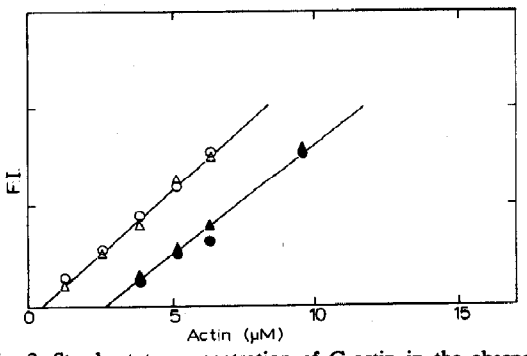

Fig. 2. Steady-state concentration of G-actin in the absence (○, △) and presence (●, ▲) of cytochalasin D (1 μM) at 31° C. 60 mM KCl, 1 mM $MgCl_2$, 50 μM $CaCl_2$, 200 μM ATP, 5 mM Tris-HCl (pH 8.0), 1 mM NaN_3, 1 mM 2-mercaptoethanol, 31° C. In order to determine the time for attaining steady-state polymerization under our experimental conditions, two kinds of starting solution were prepared: one consisting of multiply diluted G-actin (○, ●), the other of multiply diluted F-actin (△, ▲). In the first preparation (○, ●), G-actin was multiply diluted with buffer G in test tubes firstly, and then polymerized by adding KCl and $MgCl_2$ (final concentrations 60 and 1 mM, respectively). Solutions were kept at 5° C for 2 days, and the fluorescence intensity (F.I.) of each was measured after incubation for 5 h at 31° C. In other samples (△, ▲), G-actin was firstly polymerized by adding KCl and $MgCl_2$ (60 and 1 mM, respectively). After completion of polymerization, F-actin was multiply diluted in test tubes with buffer F and kept at 5° C for 2 days. Before fluorescence measurement, the solutions were incubated for 5 h at 31° C. (●, ▲) Cytochalasin D was added to each test tube (final concentration 1 μM) prior to incubation at 5° C.

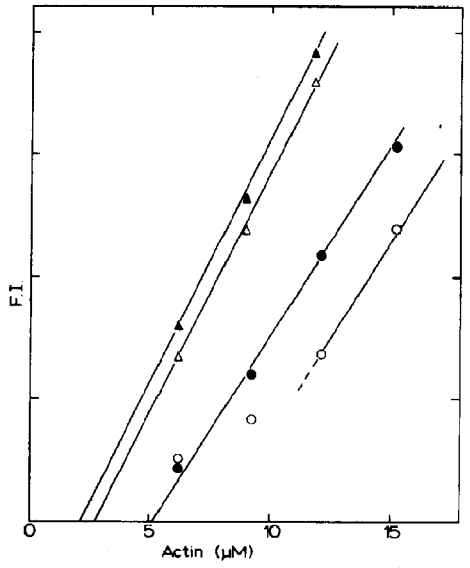

Fig. 3. Amount of F-actin as a function of total actin for various incubation times and solvent conditions at 31° C. G-Actin (5% labeled) was multiply diluted with buffer G and then polymerized by adding the following: (○, ●) 1 mM $MgCl_2$, 1 μM cytochalasin D, (△, ▲) 30 mM KCl, 1 mM $MgCl_2$, 1 μM cytochalasin D. After incubation for 5 h (●, ▲) or 25 h (○, △), the fluorescence intensity (F.I.) of each F-actin solution was measured.

4.2.2. Anomalous effect of cytochalasin D which is diminished by KCl addition; time-dependent increase in steady-state G-actin concentration

It has been reported that cytochalasin D increases the ATPase activity of actin solution [19]. Therefore, during prolonged incubation of F-actin in the presence of cytochalasin D, the ATP content decreases and that of ADP plus P_i increases gradually. Consequently, the population of ATP-G-actin decreases while that of ADP-G-actin increases. Since the steady-state concentration of

ADP-G-actin is markedly greater than that of ATP-G-actin [14], a plot of the amount of F-actin vs. total actin concentration had an upward curvature and the steady-state G-actin concentration was difficult to determine. The shift depends strongly on temperature. We confirmed this effect of cytochalasin D at 31°C as shown in fig. 3. Our significant finding is that this effect of cytochalasin D became less evident when KCl was included in the solution.

Another important recent finding which is relevant to the present study was that addition of P_i to ADP-F-actin solution reduced the critical concentration of the P-end [12,20]. This effect of P_i is explained in such a way that P_i binds to the terminal subunit at the P-end forming an actin-ADP-P_i structure whose critical concentration is lower than that of ADP-F-actin.

In summary, subunit exchange at the terminal of F-actin depends on the nucleotide (ATP or ADP or ADP plus P_i) binding to both terminal subunits as well as to the G-actin free in solution. It is important to note that, under the steady-state conditions in the presence of ATP, the nucleotide bound to the terminal subunit of F-actin varies between ATP, ADP or ADP plus P_i in a stochastic manner, and uncertainty in the nucleotide bound to the terminals is inevitable. Therefore, the rate of label incorporation determined in the present study is an average of the heterogeneous population. In the following experiments on the rate of label incorporation, we dialyzed F-actin solutions vs. ATP solution (200 μM) at 31°C in order to control the initial concentration of ATP just prior to label addition.

4.2.3. Steady-state G-actin concentration in the presence of tropomyosin

The results (table 1) show that tropomyosin did not affect the steady-state concentration of G-actin appreciably in the absence of cytochalasin D, in accordance with the results of Lal and Korn [21]. However, the effect of tropomyosin was quite evident at the P-end (in the presence of 1 μM cytochalasin D). In the presence of tropomyosin, the critical concentration of P-end was reduced from 4.7 to 1.6 μM in 1 mM $MgCl_2$ solution. Also, in a solution of 1 mM $MgCl_2$ and 30 mM KCl, it was reduced from 2.3 to 1.0 μM. This effect of tropomyosin on the P-end was not studied by the above-mentioned authors [21].

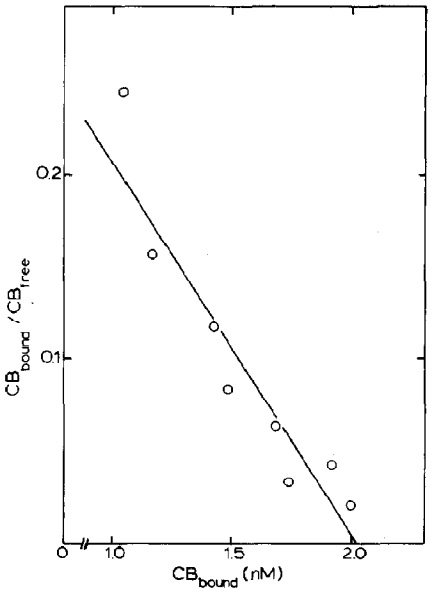

Fig. 4. Scatchard analysis of [^{3}H]cytochalasin B (CB) binding to F-actin. F-Actin (10 μM) solution containing 20 mM KCl, 1 mM $MgCl_2$, 20 mM Tris-HCl (pH 8.0), 100 μM $CaCl_2$, 200 μM ATP, 1 mM NaN_3 and 0.5 mM 2-mercaptoethanol was incubated at 30°C for 20 min. [^{3}H]Cytochalasin B (0.29 μCi/ml) was added as its final concentration between 4 and 100 nM. From Scatchard analysis (eq. 22) $n = 2.0$ nM and $K_d = 4.9$ nM were obtained.

4.3. Binding of cytochalasin B to pure F-actin

The amounts of free cytochalasin B (CB_{free}) and actin-bound cytochalasin B (CB_{bound}) were analysed according to the following relation:

$$\frac{CB_{bound}}{CB_{free}} = \frac{1}{K_d}(n - CB_{bound}) \qquad (22)$$

where n denotes the concentration of binding sites for cytochalasin B and K_d the dissociation constant of the sites. A typical plot was linear, from which we obtained $n = 2.0$ nM and $K_d = 4.9$ nM (fig. 4). Since the solution contained 10 μM F-actin, every 5000 actin subunits bind one cytochalasin B molecule on average. According to the helical structure of F-actin, 5000 actin subunits

correspond to F-actin of approx. 14 μm in length. This is a little greater than the average length of F-actin so far observed using electron microscopy and other methods [22–24]. However, taking into account differences in experimental conditions between the present and previous studies, it seems reasonable to consider the average length and concentration of F-actin used in the present study to be approx. 14 μm and approx. 2 nM, respectively. These results are compatible with the conclusion in a previous report [24]. The concentration of F-actin thus obtained was used for calculation of the on/off rate constants (table 1).

4.4. Rate of label incorporation at both ends of F-actin

As shown in table 1, the steady-state concentration of G-actin was appreciably lower than the critical concentration of the P-end. Then, by limiting the amount of label added so as to obey the condition $C_s + C_0 < C_P$, we measured the rate of label incorporation into the B-end of F-actin (case B, eq. 18). In determination of the on/off rate constants of the P-end by the use of cytochalasin D, we need to minimize the effect of the gradual shift of C_P due to accumulation of P_i in the solution [12]. For this purpose, we adopted the following experimental procedure. After attainment of a steady state for F-actin solution, the B-end of F-actin was capped by cytochalasin D (0.5 μM). As soon as capping of the B-end was completed, labeled G-actin was added and its incorporation into the P-end was followed by measuring the fluorescence increase. Under our experimental conditions, the effect of capping of the B-end reached completion within about 2 min after addition of cytochalasin D (fig. 5). Therefore, we added labeled G-actin 2 min after mixing of cytochalasin D with F-actin. It is apparent that via this procedure, the total G-actin concentration ($C(0)$) immediately after addition of labeled G-actin is approximated by ($C_s + C_0$) instead of ($C_P + C_0$). The rate of label incorporation was obtained by using eq. 21. In order to obtain k_P^+ and k_P^-, the observed incorporation was plotted as a function of $C_s + C_0$. In table 1, the values of k_P^+ and k_P^- thus obtained are compared with those

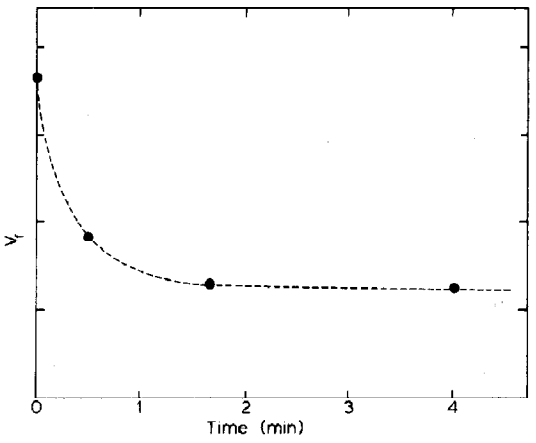

Fig. 5. Capping time of the B-end of F-actin. To 2 ml F-actin solution (10 μM) in which steady-state polymerization was established at 31° C, cytochalasin D was added to give a final concentration of 0.5 μM. After various time intervals, labeled G-actin (3 μM) was added and the initial rate of fluorescence increase V_f (label incorporation) was determined. The plateau level of V_f which indicated completion of the capping of the B-end by cytochalasin D appeared about 2 min after addition of cytochalasin D. 30 mM KCl, 1 mM $MgCl_2$, 200 μM ATP, 10 mM Tris-HCl (pH 8.0), 1 mM NaN_3, 1 mM 2-mercaptoethanol.

resulting from calculation using eqs. 19 and 20. These values are in a good agreement indicating that both ways provide good approximations of k_P^+ and k_P^-.

4.4.1. Effect of KCl

In fig. 6 and table 1, we note that in the solution of 1 mM $MgCl_2$, addition of KCl (30 mM) increased both k_B^+ and k_B^- in the same proportion so that the critical concentration C_B remained constant within experimental error. The KCl effect of acceleration of both on and off rates was also observed at the P-end. However, the increase was weaker in k_P^- resulting in a decrease in the critical concentration C_P.

4.4.2. Anisotropic constraint exerted by tropomyosin

One of the remarkable effects of tropomyosin was that it accelerated both on and off rates of the B-end, whereas it suppressed both rates for the P-end (table 1 and fig. 7). It is also interesting that tropomyosin reduced C_P remarkably while it increased C_B. Even with these changes in critical

Table 1

Kinetic parameters for subunit exchange of F-actin under steady-state conditions

C_s, steady-state concentration of G-actin. C_B[rate], C_P[rate] and C_s[rate] were calculated values from k_B^+, k_B^-, k_P^+ and k_P^- obtained experimentally according to eqs. 5, 6 and 3, respectively.

Parameters	Sample				
	Pure F-actin		F-Actin-tropomyosin		
	$MgCl_2$ (1 mM)	$MgCl_2$ (1 mM) + KCl (30 mM)	$MgCl_2$ (1 mM)	$MgCl_2$ (1 mM) + KCl (30 mM)	$MgCl_2$ (1 mM) + KCl (60 mM)
k_B^+ (M^{-1} s^{-1}) ($\times 10^6$)	3.0	6.3	5.2	6.4	6.7
$k_B^+ C_s$ (s^{-1})	2.0	3.4	2.3	2.9	2.7
k_B^- (s^{-1})	0.63	1.3	2.0	2.5	2.3
C_B[rate] (μM)	0.21	0.20	0.40	0.39	0.35
k_P^+ (M^{-1} s^{-1}) ($\times 10^6$)	0.31	1.1	0.19	0.63	1.2
$k_P^+ C_s$ (s^{-1})	0.21	0.63	0.08	0.28	0.47
k_P^- (s^{-1})	1.6	2.7	0.31	0.63	0.83
C_P[rate] (μM)	5.0	2.4	1.6	1.0	0.6
C_P (μM)	4.7	2.3	1.6	1.0	0.8
C_s[rate] (μM)	0.66	0.54	0.44	0.44	0.40
C_s (μM)	0.55	0.50	0.45	0.47	0.42
Flow (s^{-1})	1.4	2.1	0.3	0.4	0.4

concentrations of the two ends, the steady-state G-actin concentration was not as strongly influenced. This indicates that regulation of the

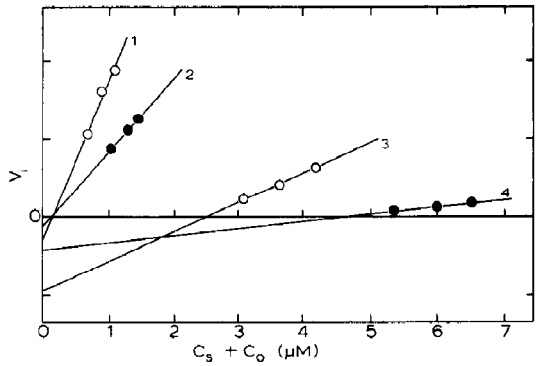

Fig. 6. Initial rate of label incorporation for F-actin in the absence and presence of cytochalasin D (0.5 μM) at 31° C. In the absence of cytochalasin D: (1) 30 mM KCl, 1 mM $MgCl_2$, (2) 1 mM $MgCl_2$; in the presence of cytochalasin D (0.5 μM): (3) 30 mM KCl, 1 mM $MgCl_2$, (4) 1 mM $MgCl_2$. Other solvent conditions: 200 μM ATP, 5 mM Tris-HCl (pH 8.0), 1 mM NaN_3, 1 mM 2-mercaptoethanol. In cases 1 and 2, V_i $[\{dFI(t)/dt\}_{(t\to 0)}/A(0)]$ was determined by using eq. 18, and in the cases of 3 and 4, eq. 21 was used.

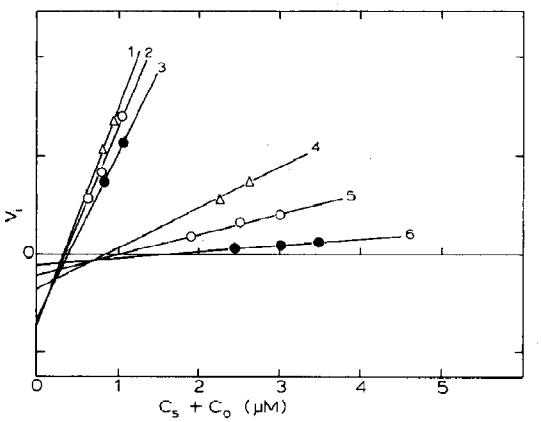

Fig. 7. Rate of label incorporation of F-actin/tropomyosin complex in the absence and presence of cytochalasin D (0.5 μM) at 31° C. In the absence of cytochalasin D; (1) 60 mM KCl, 1 mM $MgCl_2$, (2) 30 mM KCl, 1 mM $MgCl_2$, (3) 1 mM $MgCl_2$. In the presence of cytochalasin D (0.5 μM); (4) 60 mM KCl, 1 mM $MgCl_2$, (5) 30 mM KCl, 1 mM $MgCl_2$, (6) 1 mM $MgCl_2$. Other conditions as in fig. 6. In the case of 1 and 2, the total G-actin concentration ($C_s + C_0$) exceeded the critical concentration of P-end (C_P). Therefore in the calculation of k_B^+ and k_B^-, the correction was made for the contribution of the P-end by using eqs. 15 and 16.

Table 2

Steady-state ATPase activity of F-actin and F-actin-tropomyosin complex (at 31° C, 1 mM $MgCl_2$, 200 μM ATP, 10 mM Tris-HCl, pH 8.0)

20 ml F-actin (10 μM) and F-actin-tropomyosin complex (10 μM F-actin) were preincubated separately at 31° C for 2 h, and the contents of ATP and ADP in each solution were analysed. To one half of the solution, cytochalasin D was added to 1 μM, and the solutions were further incubated at 31° C. After incubation for 200–250 min, protein in 2 ml of each solution was centrifuged down, and the nucleotide contents in the supernatant were determined. The apparent rate of the ATPase (k_{app}) was calculated according to: $[ATP(t)] = [ATP(0)]\exp(-k_{app}t)$. The apparent rate was converted to the average rate of single F-actin (or F-actin-tropomyosin).

Proteins	ATPase (per F-actin) activity (s^{-1})
Pure F-actin	1.2
+1 μM cytochalasin D	4.2
F-Actin-tropomyosin	2.6
+1 μM cytochalasin D	1.0

dynamic polarity of F-actin was controlled by tropomyosin under conditions where the free energy change of polymerization is conserved [25]. This principle was also applicable to the effect of KCl (table 1). The meaning of these findings is not well understood as yet. From the present results, the most significant effect of tropomyosin binding on subunit flow in F-actin appeared in the outflow of actin subunits at both terminals. At the B-end, the terminal subunit readily underwent dissociation from the filament (k_B^- increased approx. 2-fold), while at the P-end k_P^- is reduced significantly (table 1).

4.5. Activation of steady-state ATPase activity of F-actin due to tropomyosin binding

Associated with these changes in subunit flow by lateral binding of tropomyosin, the steady-state ATPase of the solution was activated. However, when cytochalasin D (1 μM) was present in the solution, ATPase activation due to tropomyosin binding disappeared. As shown above, cytochalasin D alone activated ATPase activity of pure F-actin. We can summarise the above such that either tropomyosin or cytochalasin D was bound to F-actin with the ATPase activity of F-actin being enhanced. However, when both tropomyosin and cytochalasin D were present together, their effects were canceled out (table 2). The complexity of these effects should be clarified after further experiments.

5. Discussion

5.1. Comparison with data obtained by electron microscopic observations

Firstly, Pollard and Mooseker [2] determined the on/off rate constants of actin subunits at both ends using microvillar core bundles from electron microscopic observations. Bonder et al. [26] and

Table 3

Kinetic parameters for subunit exchange of F-actin from electron microscopy

Parameters	Samples			
	Microvillar core bundles [a]		Acrosomal bundles	
	KCl (20 mM)	$MgCl_2$ (5 mM) + KCl (75 mM)	$MgCl_2$ (5 mM) [b] + KCl (75 mM)	$MgCl_2$ (1 mM) [c] + KCl (100 mM)
k_B^+ ($M^{-1}\,s^{-1}$) ($\times 10^6$)	5.9	8.8	12.9	3.4
k_B^- (s^{-1})	6.0	2.0	3.5	0.32
k_P^+ ($M^{-1}\,s^{-1}$) ($\times 10^6$)	0.8	2.2	1.4	0.26
k_P^- (s^{-1})	0.7	1.4	0.5	0.27

[a] Data from ref. 2.
[b] Data from ref. 27.
[c] Data from ref. 28.

Coluccio and Tilney [27] also determined the rate constants using acrosomal bundles in electron microscopic observations. These rate constants from electron microscopic observations are presented in table 3. The previous data are comparable to those obtained in the present study using fluorescence methods (table 1). The fluorescence methods developed here provide excellent results as regards the detectable threshold (a few subunits associated at the terminal in the fluorescence method and growth of as little as 10 monomers in electron microscopic observations [26,27]) and the ease of tracing the time course of subunit association.

5.2. Experimental error

The present fluorescence method for determination of on/off rate constants of actin subunits at each end of F-actin has some inevitable experimental errors.

As described in section 2.5, we analyzed the rate of label incorporation by using eq. 10 (not eq. 10′) with the rate of the fluorescence increase being averaged over the time domain between 50 and 120 s after addition of labeled G-actin. In this time domain, $A(0)$ (the fraction of labeled G-actin) and $C_s + C_0$ (total G-actin) are lower than their initial values used in eqs. 15, 16, 18 and 21. The extents of the decrease in these parameters were checked by computer simulation (see appendix A and table 5) and found to have a range of unavoidable error of several percent to tens of percent.

In determination of on/off rates at the P-end, cytochalasin D was used. This gives rise to another form of experimental error. As described in section 4.4, we added labeled G-actin 2 min after mixing cytochalasin D with F-actin. After capping of the B-end with cytochalasin D, the monomer concentration began to increase from its initial value C_s to C_P. Our results in fig. 5 suggest that the capping of the B-end of F-actin by cytochalasin D was not a rapid process. Therefore, in the most extreme case (pure F-actin, 1 mM $MgCl_2$ and 30 mM KCl), the extent of the increase in monomer concentration will be no greater than 50% of the value of C_s 2 min after addition of cytochalasin D. This increase in monomer amounts to about 10% of $C_s + C_0$ in eqs. 16 and 21. This error is also unavoidable.

From the above, we estimated the rate constants obtained to include about 10–15% error.

5.3. Subunit flow in F-actin

In fig. 8, the present results are summarized in terms of the steady-state subunit flow in F-actin. It is apparent that in pure F-actin net subunit flow occurs in the direction from the B- to P-end. In the case of 1 mM $MgCl_2$, the rate of net flow was 1.4 subunits/s. Associated with this subunit flow, the free energy of ATP bound to ATP-G-actin is transformed into the free energy of F-actin. The steady-state rate of ATPase was approximately the same as the net subunit flow (table 2). When KCl was added to give a concentration of 30 mM, the net rate of subunit flow increased to 2.1 subunits/s.

Binding of tropomyosin had a surprising effect on the subunit flow. The rate of dissociation at the P-end was reduced to 1/3–1/4 of that of pure F-actin, while at the B-end it increased to 2–3-fold that of pure F-actin. As a consequence, net subunit flow from the B- to P-end was reduced to about 0.3 subunit/s (in 1 mM $MgCl_2$). This effect is due to stabilization of F-actin. However, it should be pointed out that the dynamic polarity of F-actin was enhanced by binding of tropomyosin; i.e., the total (on + off) frequency at the B-end increased on binding of tropomyosin, while that at the P-end was reduced. This indicates that structural fluctuation of the B-end was enhanced by tropomyosin, while that of the P-end was suppressed. It is very likely that the structural fluctuation at the B-end enhanced by tropomyosin may be related to the activation of steady-state ATPase by tropomyosin binding as described above.

5.4. Relation to the flexibility of F-actin

Our results suggest that the structural constraint exerted by the regulatory protein on the individual actin subunit is in the direction of the long axis of F-actin, directed from the P- to B-end. This directional constraint modulates the fluctuation of coupling between subunits not only at the

terminal but also in the body of F-actin. We understand that the Ca^{2+}-dependent modulation of the directional constraint must be very closely related to the Ca^{2+}-dependent change in flexibility of regulated F-actin reported previously [28]. In ref. 28, it was found that while the flexural rigidity of F-actin increases upon binding of native tropomyosin, the torsional rigidity is not significantly affected and that the flexural rigidity of F-actin becomes Ca^{2+}-sensitive when regulatory proteins bind to F-actin. The macroscopic flexural rigidity is related to the restricted rotation of actin subunits around the short axis of F-actin, while the macroscopic torsional rigidity concerns the limited rotation of actin subunits around the long axis. These two kinds of rotation of the terminal actin subunit are involved in the molecular process of dissociation of the terminal subunit.

5.5. Dynamic polarity of F-actin

For understanding of the dynamic polarity of F-actin as exemplified by the subunit flow under steady-state condition, let us consider the mode of subunit coupling in actin filaments depicted schematically in fig. 9. In this model, each subunit is represented by a skewed shape to show the intrinsic asymmetry of the subunit. This is the

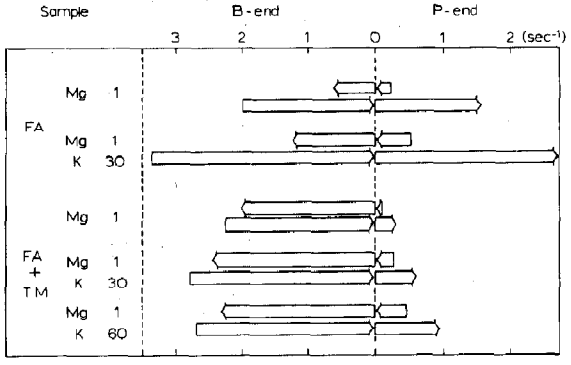

Fig. 8. Subunit-flow diagram in F-actin and F-actin-tropomyosin complex. From the on/off rate constants of the terminal actin subunit of both F-actin and F-actin-tropomyosin complex (table 1), the steady-state subunit flow in and out at the B- and P-ends was calculated according to the following relations. (B-end) $k_B^+ C_s$ (inflow), k_B^- (outflow). (P-end) $k_P^+ C_s$ (flow in), k_P^- (flow out). FA and TM denote F-actin and tropomyosin respectively, and Mg 1, K 30 and K 60 denote 1 mM $MgCl_2$, 30 mM KCl and 60 mM KCl, respectively.

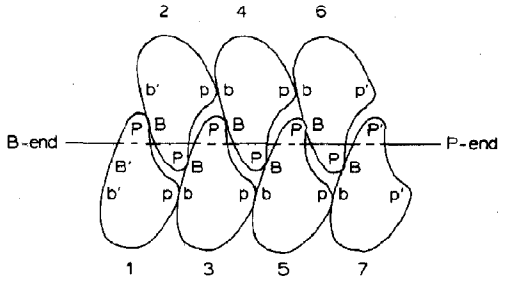

Fig. 9. Schematic illustration of the contacts between actin subunits in F-actin.

basis of the (static) polarity of F-actin as providing the means of distinction between the B- and P-ends. The individual subunit interacts with four neighbouring actin subunits, except the terminal subunits; i.e., subunits 1 and 2 at the B-end and 6 and 7 at the P-end. Clearly, the process of dissociation of subunit 1 from the B-end requires the simultaneous disruption of two bonds, P1–B2 and p1–b3. In the course of breaking these bonds, a structural change in subunit 1 will occur. The structural change may be restricted to the bonding sites P1 and p1, or may be distributed over a larger part of the subunit. Concomitantly, structural changes in subunits 2 and 3 will occur at sites B2 and b3. It is also apparent that in the process of association of subunit 1 with the B-end, a similar (but not necessarily strictly reverse) structural change will occur. On the other hand, when subunit 7 at the P-end dissociates, the two bonds B7–P6 and b7–p5 are broken simultaneously. Structural change in subunit 7 as well as in subunits 6 and 5 will be associated with this process. It is thus clear that the structural change at the terminal subunits during the course of dissociation (or the association) differs between the B- and P-ends. This disparity in dynamic structure of the terminal subunits is exemplified by the observed rate constants (table 1).

Appendix A

A1. Monte-Carlo simulation of the early stage of label incorporation after addition of labeled G-actin

Under the experimental conditions in fig. 2, C_s was apparently smaller than C_P. Therefore, we

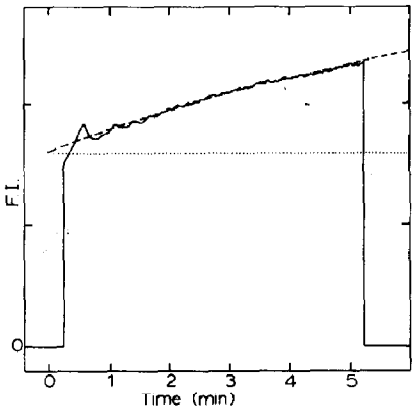

Fig. 10. Comparison of the experimental curve for label incorporation of F-actin (———) with the theoretical curve obtained by Monte-Carlo simulation (- - - - - - and · · · · · ·). The solid line is the experimental curve for increase in fluorescence intensity (F.I.) associated with label incorporation into F-actin. F-Actin (10 μM) was incubated at 20 °C for 20 min. At $t = 0$, the labeled G-actin (36% label) was added to give 0.32 μM. The fluorescence measurement was started after dead time (about 15 s). The solution contained 20 mM KCl, 1 mM $MgCl_2$, 100 μM $CaCl_2$, 100 μM ATP and 20 mM Tris-HCl (pH 8.0), 250 μM DTT and 1 mM NaN_3. (- - - - - -) Computer simulation of label incorporation at the B- plus P-ends (eq. 11); (· · · · · ·) label incorporation at the P-end only (eq. 12). Values of parameters used in simulation ($k_B^+ = 0.85 \times 10^6$ M^{-1} s^{-1}, $k_B^- = 0.53$ s^{-1}, $k_P^+ = 0.17 \times 10^6$ M^{-1} s^{-1} and $k_P^- = 0.28$ s^{-1}) were experimentally determined under the same solvent condition using eqs. 18–20. Ordinate and abscissa were transformed to the experimental scale using the proportionality constant obtained not arbitrarily but from the actual experiment.

consider here only the case of $(C_s + C_0 < C_P)$. Under this condition, the added label binds mostly to the B-end, while at the P-end dissociation of the terminal subunit (unlabeled) is the major event. The incorporation of label immediately after addition of labeled G-actin follows eq. A1 which lacks the dissociation term, since labeled G-actin is not yet in binding equilibrium:

$$V^*(t \to 0) = A(0) k_B^+ C(0) \qquad \text{(A1)}$$

As the incorporation of label proceeds and binding equilibrium of label is attained, the rate of label incorporation is described by eq. A2 which is the same as eq. 18:

$$V^*(t \to 0) = A(0)\left[k_B^+ C(0) - k_B^-\right] \qquad \text{(A2)}$$

Table 4

Change in rate of label incorporation after addition of label calculated from the simulated curve (1), and the rate of label incorporation calculated from eqs. A1 and A2 (2)

Fluorescence change expressed in (mm/s) on the chart of the recorder. We note that the rate obtained from eq. A1 was close to that averaged over the simulated curve between 0 and 1 s, and that obtained from eq. A2 was close to the average rate between 50 and 120 s.

Time interval (s)	Rate of fluorescence change (mm/s)	
	(1) Average rate (simulated curve)	(2) From eqs. A1 and A2
0– 1	0.317	0.313 (eq. A1)
4– 5	0.218	
9– 10	0.192	
20– 30	0.156	
50– 60	0.132	
110–120	0.135	0.137 (eq. A2)
170–180	0.124	
230–240	0.091	
290–300	0.101	

The time necessary for the shift of the condition from eq. A1 to eq. A2 depends on the magnitudes of k_B^+ and k_B^-. In this appendix, we examine the time domain where the incorporation of label is described by eq. A2.

A2. Algorithm

We took 1000 F-actin to represent the stochastic process of subunit exchange. In order not to lose the generality of the results, we adopt eq. 10 in the computer simulation:

$$V^*(t) = A(t)\left[\left(k_B^+ + k_P^+\right)C(t) - \left(k_B^- + k_P^-\right)\right] \qquad \text{(A3)}$$

Simulation was performed in the following sequence.

Table 5

Change in total G-actin concentration and fraction of labeled G-actin over the time domain of simulation

Time (s)	Total G-actin concentration (μM)	Fraction of labeled G-actin (%)
0	1.12	10.3
60	1.08	10.1
120	1.05	9.92

(1) The probabilities of association of G-actin with F-actin and subunit dissociation from F-actin were calculated every 0.2 s.

(2) At the i-th time of splicing, the concentration of G-actin $C(i)$ and the fraction of labeled G-actin $A(i)$ were taken as the result of simulation at the $(i-1)$-th splicing time.

(3) The amount of G-actin (labeled plus unlabeled) which associated with 1000 F-actins was calculated using $k_B^+C(i)$ and $k_P^+C(i)$, and the F-actin with which the G-actins associated was selected randomly from 1000 F-actins. Whether or not the associated G-actin was labeled was determined according to $A(i)$.

(4) The number of G-actins which dissociate from 1000 F-actins was determined using k_B^- and k_P^-, and then F-actin from which the terminal subunit dissociated was selected randomly.

(5) The total loss and gain in the G-actin pool (labeled and unlabeled) in the i-th splicing time determined $C(i+1)$ and $A(i+1)$. This sequence of calculations was repeated over 1800 cycles (6 min).

In the above calculation, the on/off rate constants and steady-state concentration of G-actin were held fixed. A number concentration of F-actin (P) equal to 2 nM was used.

A3. Time course of fluorescence increase

The average number of labeled G-actin molecules, $n(i)$, which had been incorporated into single F-actin as far as the i-th step was multiplied by fP (eq. 11). This gave the time course of the fluorescence increase due to label incorporation in the solution. The result thus obtained showed a perfect fit to the experimental curve over all time domains examined (fig. 10). Since all parameters used in the calculation were derived from the experimental results, we concluded that the analysis with this novel method gave a self-consistent result.

In order to determine the time domain appropriate for using eq. 18, the average rate of the simulated fluorescence increase was calculated for several time intervals (table 4): As expected above, the simulated rate in the very initial stage (0–1 s) coincided with eq. A1. The rate obtained by using eq. A2 was very close to the simulated values in the time domain between 30 and 150 s. These results indicate that the incorporation of labeled G-actin into the B-end of F-actin reached equilibrium within 30 s after addition of the label. This in turn indicates that our selection of the time domain at 1–2 min for applying eq. 18 was very reasonable. Also, it is shown (table 5) that when the incorporation proceeded 2 min after addition of the label, the total G-actin and labeled G-actin decreased by only 6 and 3%, respectively. This is exactly the condition that we have assumed as the requirement for quasi-steady-state analysis. The dotted line in fig. 10 indicates the simulation for incorporation of label at the P-end, showing that it was negligible relative to label incorporation at the B-end at least under our experimental conditions, i.e., $(C_s + C_0) < C_P$. This result again justifies the use of eq. 18 in our analysis.

Acknowledgement

We would like to thank Dr. H. Hayashi (Department of Molecular Biology, Nagoya University) for performing HPLC.

References

1 A. Wegner and G. Isenberg, Proc. Natl. Acad. Sci. U.S.A. 80 (1983) 4922.
2 T.D. Pollard and M.S. Mooseker, J. Cell Biol. 88 (1981) 654.
3 H. Kondo and S. Ishiwata, J. Biochem. 79 (1976) 159.
4 A. Wegner, J. Mol. Biol. 108 (1976) 139.
5 J.-M. Neuhaus, M. Wanger, T. Keiser and A. Wegner, J. Muscle Res. Cell Motil. 4 (1983) 507.
6 M. Wanger, T. Keiser, J.-M. Neuhaus and A. Wegner, Can. J. Biochem. Cell Biol. 63 (1985) 414.
7 T. Kouyama and K. Mihashi, Eur. J. Biochem. 114 (1981) 33.
8 F.B. Straub and G. Feuer, Biochim. Biophys. Acta 4 (1950) 455.
9 T.D. Pollard and A.G. Weeds, FEBS Lett. 170 (1984) 94.
10 M.-F. Carlier, D. Pantaloni and E.D. Korn, J. Biol. Chem. 262 (1987) 3052.
11 E.D. Korn, M.-F. Carlier and D. Pantaloni, Science 238 (1987) 638.
12 M.-F. Carlier and D. Pantaloni, J. Biol. Chem. 263 (1988) 817.

13 M.-F. Carlier, D. Pantaloni and E.D. Korn, J. Biol. Chem. 260 (1985) 6565.
14 T.D. Pollard, J. Cell Biol. 103 (1986) 2747.
15 S.L. Brenner and E.D. Korn, J. Biol. Chem. 254 (1979) 9982.
16 A. Satoh and K. Mihashi, J. Biochem. 71 (1972) 597.
17 K. Mihashi, J. Biochem. 96 (1984) 273.
18 S. Lin, D.Y. Santi and J. Spudich, J. Biol. Chem. 249 (1974) 2268.
19 S.L. Brenner and E.D. Korn, J. Biol. Chem. 256 (1981) 8663.
20 J.E. Rickard and P. Sheterline, J. Mol. Biol. 191 (1986) 273.
21 A.A. Lal and E.D. Korn, Biochemistry 25 (1986) 1154.
22 S.L. Brenner and E.D. Korn, J. Biol. Chem. 258 (1983) 5013.
23 T.D. Pollard, Anal. Biochem. 134 (1983) 406.
24 E. Garzi and G. Trombetta, Biochem. Biophys. Res. Commun. 139 (1986) 109.
25 F. Oosawa and S. Asakura, Thermodynamics of the polymerization of protein, eds. B. Horecker, N.O. Kaplan, J. Marmur and H.A. Scheraga (Academic Press, New York, 1975) p. 28.
26 E.M. Bonder, D.J. Fishkind and M.S. Mooseker, Cell 34 (1983) 491.
27 L.M. Coluccio and L.G. Tilney, J. Cell Biol. 99 (1984) 529.
28 K. Mihashi, A. Ooi, N. Suzuki, H. Yoshimura and K. Kinosita, Jr, Life Sci. Adv. Mol. Cell. Biol. 7 (1988) in the press.